Caractérisation et modélisation du comportement en corrosion sous contrainte intergranulaire de noyau de soudure FSW de l'alliage 2050

Matthieu Dhondt, Isabelle Aubert, Nicolas Saintier, J.M. Olive

Characterization of intergranular stress corrosion cracking behavior of a FSW Al-Cu-Li 2050 nugget

M. Dhondt[a], I. Aubert[a], N. Saintier[b], JM. Olive[a]

a. *I2M, UMR 5295, Université de Bordeaux, CNRS, 351 Cours de la Libération, Talence, 33405 France*

b. *I2M, UMR 5295, Arts et Métiers Paris-Tech (Centre de Bordeaux-Talence), Esplanade des Arts et Métiers, Talence, 33405 France*

Résumé :

Cette étude est dédiée au comportement en corrosion sous contrainte d'un alliage Al-Cu-Li 2050 soudé par FSW et s'inscrit dans le cadre de l'allègement des structures aéronautiques. En service, les structures soudées peuvent être soumise à la fois à des contraintes mécaniques et à un environnement agressif. L'objectif de cette étude est de caractériser le comportement en corrosion sous contrainte (CSC) du noyau de soudure FSW de l'alliage 2050. Dans un premier temps, un lien est établi entre les hétérogénéités de microstructure induites par le procédé de soudage et les champs mécaniques locaux se développant lors d'un essai de traction, puis, entre ces hétérogénéités et le développement de fissures de CSC-IG du noyau de soudure.

Abstract :

This study deals with the in service durability of an alloy Al-Cu-Li 2050 friction stir welded. In an aeronautical context, this material could be submitted to mechanical stresses and a corrosive environment. Thus, the aim of this study is to characterize the intergranular stress corrosion cracking (IGSCC) behavior of the 2050 FSW weld nugget. Firstly, a link has been established between several microstructural heterogeneities induced by the welding process and local strain variations, then between these heterogeneities and the initiation and propagation of IGSCC cracks.

Mots clefs : Alliage d'aluminium ; Friction stir welding ; Corrosion sous contrainte intergranulaire

1 Introduction

Friction stir welding (FSW) is a solid state metal joining technique for joining aluminum alloys, even those that are typically considered to be un-weldable, such as aluminum alloys 2XXX and 7XXX. Using both lightweight aluminum lithium alloy and FSW technique could decrease significantly the weight of aircraft structures. The FSW process generates strong microstructural changes due to the high plastic deformation and the frictional heat induced by the rotating tool. Friction stir welded joints consist of three zones involving specific microstructures [Pouget2008, Proton2011, Bousquet2011] namely : heat affected zone (HAZ), thermo-mechanically affected (TMAZ) zone and weld nugget (WN).

Some works showed that friction stir-welded joints of alloys AA2050, AA2024 and AA7050, exhibit susceptibility to localized corrosion compared to the base metal [Proton2011, Bousquet2011, Lumsden2003], and Bousquet [Bousquet2011] highlighted a transition between pitting corrosion in base metal of alloy 2050 and intergranular corrosion (IGC) in the weld nugget. For alloys Al-Cu-Li, the localized corrosion susceptibility can be correlated with precipitates T1 (Al_2CuLi), due to the potential difference between the precipitates and the matrix [Buchheit90, Li2008]. With regard to IGC, it has been found to be strongly dependent on the crystallographic nature of the grain boundaries

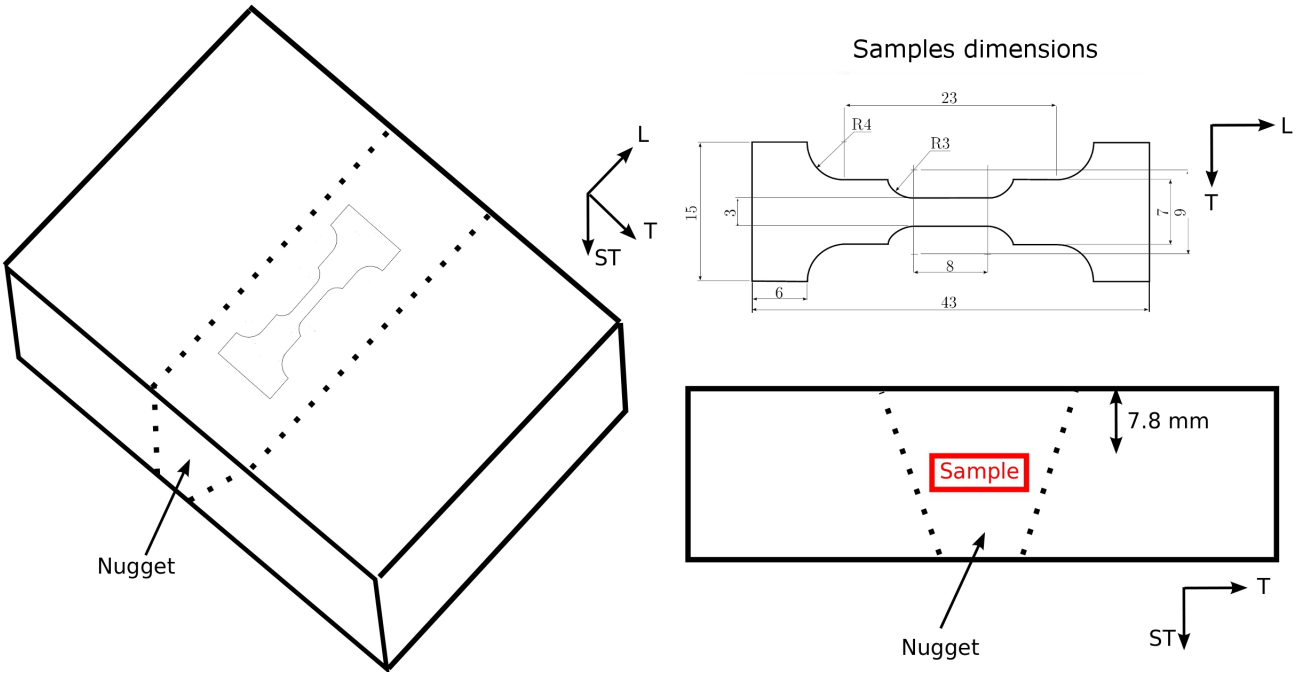

FIGURE 1 – Tensile samples machining

[Kim2001, Arafin2009]. But in the case of this study, not only grain boundary character distribution but also the mechanical fields play a key role. For AA2024, applying an internal stress [Liu2004], or an external stress [Pauze2008] causes an increase of the IGC growth rate.

The intergranular stress corrosion cracking (IGSCC) being strongly correlated with the microstructure and particularly precipitates, it can be improved by heat treatments after welding. Recently, Proton *et al.* [Proton2011] highlighted that a post-welding heat treatment improves the resistance to environmental degradation of 2050 FSW joints. In this study, we will focus on the post-welding heat-treated weld nugget of AA2050, which is the preferential IGSCC initiation zone of the friction stir-welded joint. The effects of microstructure heterogeneities on local mechanical fields and their consequences on the IGSCC behavior have been investigated.

2 Material and methods

The weld nugget used in this study, comes from the friction stir welding of two 15 mm thick sheets of AA2050 T3 (solutionising, quenching and stretching), followed by a post-welding heat treatment at 155°C. Tensile samples were machined in the middle of the nugget, along the welding direction (figure 1).

To establish a correlation between crystallographic texture and local strain heterogeneities, EBSD cartographies of about 1500 X 400 μm with a step of 2 μm were performed using a OIM EBSD system on a ZEISS EVO50 scanning electron microscopy (SEM) along the gauge length of samples previously mechanically polished to a mirror finish (1/4 μm OP-S solution). Then, the samples were electrolytically etched in a HBF4 solution with an intensity of 0.2 A.cm^{-2} during 2 min, to create a texture used to measure displacement fields by Digital Images Correlation (DIC) during the tensile test. *In-situ* tensile tests in air were performed at $\dot{\epsilon} = 5.10^{-5}$ s^{-1} total strain rate under a numeric microscope KEYENCE VHX-1000E. Strain gauge provided the strain in the range of 0 to 2 %. Above 2 %, strain was estimated thanks to LVDT displacements measurements. The local strain fields were estimated by DIC using the software Correli^{Q4}, from 300 optical images taken every 15 s (for a $\Delta\epsilon = 7.5.10^{-4}$) during the tensile test. The investigated area for DIC measurements of about 1600 X 1200 μm contained the EBSD cartography zone. In addition, some corrosion tests were performed to link the IGSCC cracks initiation with the heterogeneities of microstructure and the mechanical fields.

Corrosion tests were realized on samples mechanically polished to a mirror finish (1 μm diamond paste). All the corrosion tests were performed in a 1.0 M NaCl aerated solution at Open Current Potential and at room temperature, the immersion duration being fixed to 1h30. In order to underline an eventual internal and external stress effect on IGSCC, three types of tests were conducted :

– corrosion tests (COR) by immersion in NaCl,
– stress corrosion cracking tests (SCC) by application of an external loading during immersion in NaCl,
– corrosion tests by immersion in NaCl of samples previously pre-strained in air(PRE) to show the influence of residual stress.

To clearly evaluate the external stress effect on corrosion behavior, corrosion tests were performed on the samples previously submitted to SCC tests, by immersion of the heads of the tensile samples, which were nor mechanically nor electrochemically affected during the SCC test. SCC tests were conducted at $\dot{\epsilon} = 2.10^{-6}$ s^{-1} strain rate. The corrosive solution was added at a stress higher than the yield stress in order to limit pitting phenomenon. The immersion duration of 1h30 corresponded to 1 % of plastic strain. For corrosion tests on pre-strained samples, a traction test in air was performed at $\dot{\epsilon} = 5.10^{-5}$ s^{-1} up to 10 % of plastic strain before immersion in NaCl solution. After the tests, the SCC cracks were observed using an optical microscope OLYMPUS PMG3 and on a scanning electron microscope (SEM) JEOL 840A. After the SCC tests, samples were mechanically polished with an OP-S solution (1/4 μm), and EBSD cartographies were performed to highlight a correlation between IGSCC-cracks and the microstructure.

3 Results

3.1 Relationship between microstructure and local strain heterogeneities

Tensile tests performed on the weld nugget samples allow underlining significant strain heterogeneities as shown on the optic image (figure 2(a)). To quantify those local strain heterogeneities, DIC measurements were performed from the *in-situ* optic images taken during the tensile test. The cartography corresponding to local total strain in the tensile direction ϵ_{TT} at the specimen surface after 7 % of global strain is shown in figure 2(b). As expected, strain heterogeneity follows the dark bands observed on the optic image, the relative variation is about 15% between the maximum and the minimum ϵ_{TT} strain at the surface. The EBSD cartography previously carried out in the same zone is also shown and allows highlighting periodic crystallographic texture variations. The characteristic average band width formed by this texture was measured to be approximately 500 μm, which corresponds to the FSW tool advance per revolution. This microstructure corresponds to the typical "onion rings" structure of the FSW weld nugget [Fonda2007]. Compared to EBSD with DIC measurements, a good correlation is established between the strain heterogeneities and the crystallographic texture variation. "Onion rings" microstructure is mainly responsible for the strain heterogeneities of this material.

3.2 Intergranular stress corrosion cracking (IGSCC)

3.2.1 Stress effect

For each corrosion test, a SEM image characterizing corrosion features of the material is shown in figure 3. Those pictures show that the weld nugget is sensitive to pitting corrosion when it is not submitted to a mechanical loading (figure 3(a)). A mechanical loading induces a change in corrosion features, damage by IGSCC becomes predominant even if pitting corrosion is still present (figures 3(b) and 3(c)). The same type of phenomenon was observed by Connolly and Scully [Connolly2005] for a alloy Al-Li-Cu 2096. Those observations clearly underline the fact that an (internal or external) stress is required to produce initiation of IGSCC for those conditions (immersion duration, solution, temperature ...).

IGSCC features also depend on nature (external or internal) of the stress application. For SCC tests, cracks mainly propagate perpendicularly to the tensile direction (figure 3(b)). For corrosion tests on

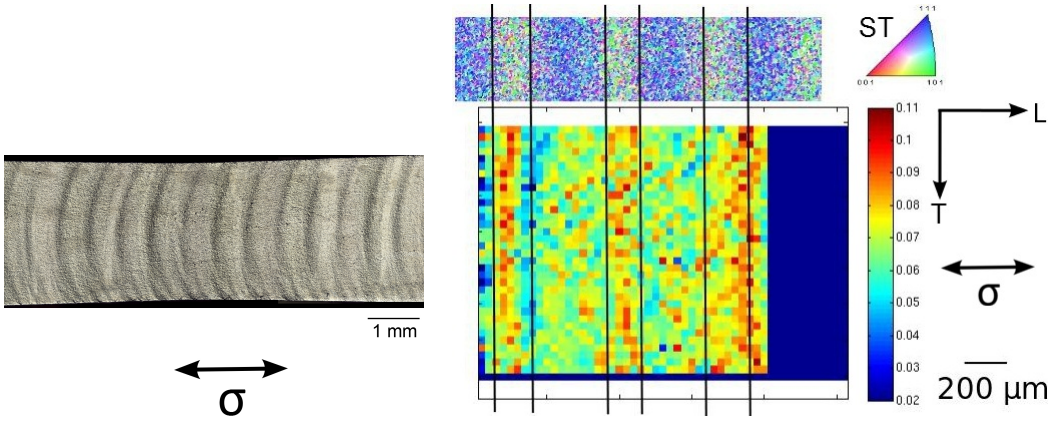

(a) Optic image after tensile test (b) Correlation between DIC measurements and EBSD cartographies

FIGURE 2 – Underlining of local strain heterogeneities on optic image and DIC measurements after 7 % of global strain

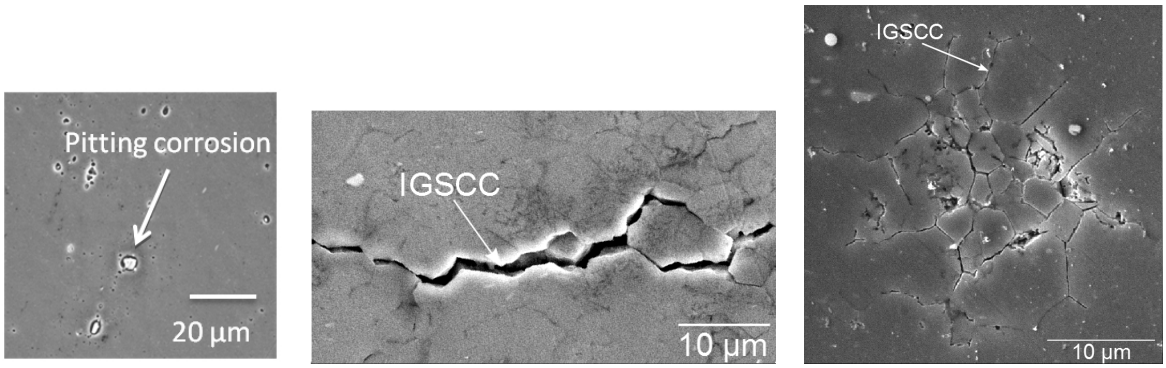

(a) *COR* (b) *SCC* (c) *PRE*

FIGURE 3 – SEM images taken after (a) a corrosion test (b) a SCC test (c) a corrosion test on a pre-strained sample

pre-strained samples, no macroscopic stress is applied, but plastic strain induced by the mechanical loading, performed before immersion generate residual local stress (due to intergranular strain incompatibilities). In this case, development of IGSCC cracks is isotropic, they have no preferential propagation directions as shown in figure 3(c).

In the following of this document, the study will be focused on the SCC tests which corresponds to the most critical situation. SEM observations reveal initiation of several cracks whose lenghts and locations are distributed. A statistical analysis of the area shown in figure 4(a) highlights that the crack density is about 168 cracks per mm^2. The crack lengths distribution is shown in figure 4(b) and the crack length average is 20 μm. In this figure, the length of more than 50 % of the cracks is lower than 10 μm. However, the length of a slight fraction ($\sim$ 2 %) of them is higher than 100 μm. We can see on the optical image (figure 4(a)), that the cracks seem to appear periodically. The correlation with microstructure is investigated in the next section.

3.2.2 Microstructure effect at mesoscopic scale

To establish a possible relationship between periodic texture variation and IGSCC initiation, EBSD cartographies were performed next to the biggest intergranular cracks shown in figure 4(a). Figure 5 clearly shows those cracks initiate at texture bands boundaries. Strain incompatibilities generated by crystallographic texture create some preferential sites for IGSCC initiation. However, texture variation is not the only parameter influencing IGSCC and smaller intragranular cracks uniformly initiate on

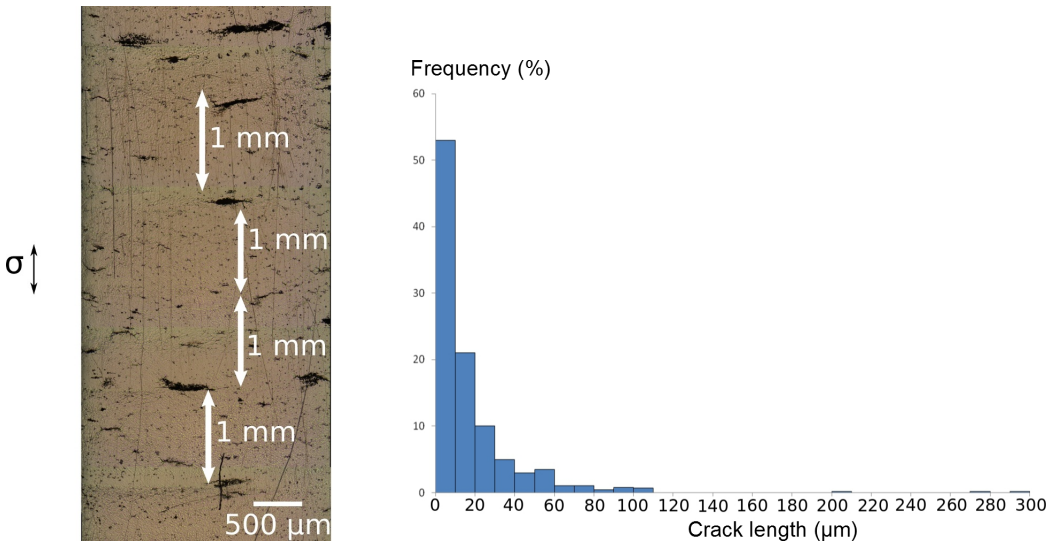

(a) Optic image of a sample submitted to an IGSCC test

(b) Crack length distribution in the sample

FIGURE 4 – Optic image and crack length distribution after IGSCC test

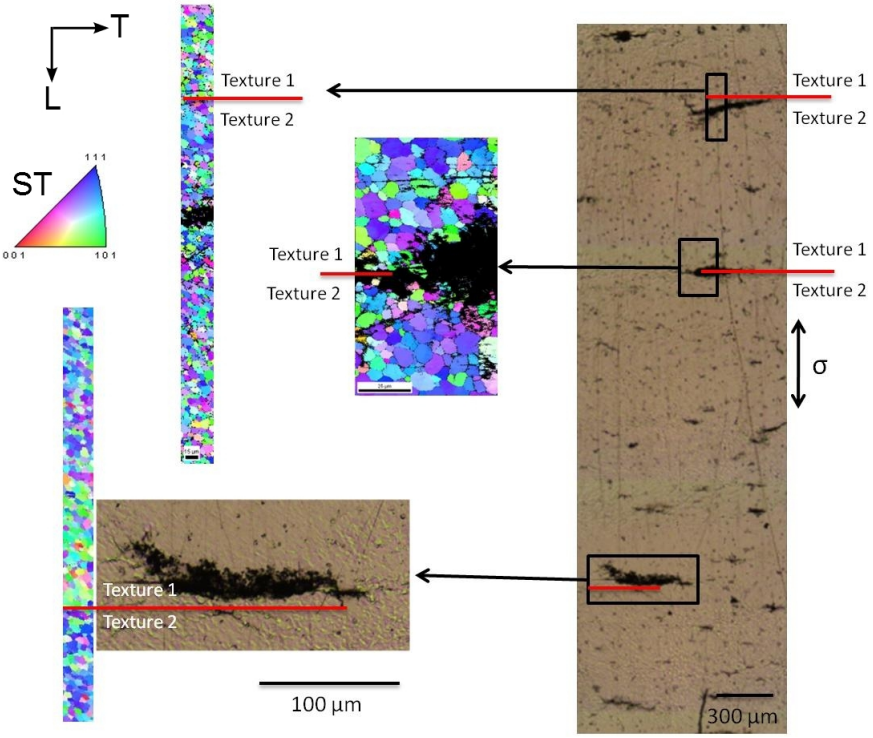

FIGURE 5 – Optic image of sample which was submitted to IGSCC test and EBSD cartographies performed next to the cracks

all the sample. Crack initiation can also depend on local mechanical fields and local microstructure (precipitation, grain boundary misorientations ...). On the other hand, the frequency of the biggest crack is two times lower than the texture band periodicity. IGSCC initiation causes a stress relaxation in the crack plane, which reduces the initiation probability at the neighboring texture band.

4 Conclusions

Under severe experimental coupled environmental and mechanical conditions, IGSCC initiates, without pitting, at grain boundaries of 2050 FSW weld nugget. Initiation stage is shown to be strongly dependent on mechanical and microsctructural parameters at mesoscopic scale. At this scale, a periodical variation of grains crystallographic orientations and associated strain heterogeneities were identified experimentally by combining EBSD and digital image correlation technique. It is evidenced that stress corrosion cracks initiate and propagate preferentially along the boundaries between textured bands. At macroscopic scale, under stress corrosion cracking conditions, multi-cracking process occurs and leads to the degradation of the material. Without any residual stress or macroscopic applied stress, a slight degradation in the form of pitting corrosion develops without any intergranular corrosion.

5 Acknowledgments

This work was financially supported by the National Research Agency (ANR) project MatetPro program ANR-08-MAPR-0020-05 (Coralis project, Corrosion of Aluminium Lithium Structures).

Références

[Arafin2009] Arafin, M.A., Szpunar, J.A. 2009 A new understanding of intergranular stress corrosion cracking resistance of pipeline steel through grain boundary character and crystallographic texture studies. *Corros. Sci.* **51** 119-128

[Bousquet2011] Bousquet, E. 2011 Durabilité des assemblages soudés par friction stir welding (FSW). Corrélation entre microstructure et sensibilité à la corrosion. *Ph.D. thesis, Université Bordeaux 1*

[Buchheit90] Buchheit Jr.,R. G., Moran,J. P., Stoner,G. E. 1990 Localized corrosion behavior of alloy 2090. The role of microstructural heterogeneity. *Corrosion.* **46** 610-617

[Connolly2005] Connolly, B.J., Scully, J.R. 2005 Transition from localized corrosion to stress corrosion cracking in an Al-Li-Cu-Ag alloy. *Corrosion.* **61** 1145-1166

[Fonda2007] Fonda, R.W., Bingert, J.F. 2007 Texture variations in an aluminum friction stir weld. *Scripta Mater.* **57** 1052-1055

[Kim2001] Kim, S.H., Erb, U., Aust, K.T., Palumbo, G. 2001 Grain boundary character distribution and intergranular corrosion behavior in high purity aluminum. *Scripta Mater.* **44** 835-839

[Li2008] Li, J.F., Li, C.X., Peng, Z.W., Chen, W.J., Zheng, Z.Q. 2008 Corrosion mechanism associated with T1 and T2 precipitates of Al-Cu-Li alloys in NaCl solution. *J Alloys Compd.* **460** 688-693

[Liu2004] Liu, X., Frankel, G.S., Zoofan, B., Rokhlin, S.I. 2004 Effect of applied tensile stress on intergranular corrosion of AA2024-T3. *Corros. Sci.* **46** 405-425

[Lumsden2003] Lumsden, J.B., Mahoney, M.W., Rhodes, C.G., Pollock, G.A. 2003 Corrosion behavior of friction-stir-welded AA7050-T7651. *Corrosion.* **59** 212-219

[Pauze2008] Pauze,N. 2008 Fatigue corrosion dans le sens travers court de tôles d ?aluminium 2024-T351 présentant des défauts de corrosion localisée. *Ph.D. thesis, École Nationale Supérieure des Mines de Saint-Etienne*

[Pouget2008] Pouget, G., Reynolds, A.P. 2008 Residual stress and microstructure effects on fatigue crack growth in AA2050 friction stir welds. *Int J Fatigue.* **30** 463-472

[Proton2011] Proton, V., Alexis, J., Andrieu, E., Blanc, C., Delfosse, J., Lacroix, L., Odemer, G. 2011 Influence of post-welding heat treatment on the corrosion behavior of a 2050-T3 aluminum-copper-lithium alloy friction stir welding joint. *J Electrochem Soc.* **158** C139-C147